Polymer Testing 98 (2021) 107201

Contents lists available at ScienceDirect

Polymer Testing

journal homepage: http://www.elsevier.com/locate/polytest

New non-destructive optical approach to determine the crystallization kinetics of PLA under a CO2 atmosphere with spatial and temporal resolution

J. Martín-de León *, V. Bernardo, E. Solórzano, M.A. Rodriguez-Pérez

Cellular Materials Laboratory (CellMat), Condensed Matter Physics Department, University of Valladolid, Valladolid, 47011, Spain

ARTICLE INFO

Keywords:
PLA
Crystallization kinetics
CO2
Avrami

ABSTRACT

The kinetics of crystallization of Polylactic Acid (PLA) in the presence of CO_2 pressures from 1.5 to 4 MPa, has been studied by measuring the optical absorbance evolution of the material with time. To perform this study, an own-designed pressure vessel provided with windows has been used. The non-destructive approach presented in this paper allows for obtaining very accurate crystallinity data as a function of time for a wide range of pressures. Besides, this new approach allows measuring with spatial resolution, i.e., obtaining the crystallization kinetics' evolution in different areas of the samples, which helps to analyze in detail the crystallization mechanisms by using the Avrami approach. The results obtained have allowed observing an unexpected peak in the absorbance curve connected with the physical phenomena taking place during the CO_2 uptake and the associated crystallization of PLA.

1. Introduction

Polystyrene (PS) foams (both expanded and extruded (EPS and XPS)) have been widely used in commodity applications such as cushioning, plastic utensils, and especially in food packaging, packaging of electronic products, and thermal and acoustic insulation applications in the building industry [1].

European Union estimated the total amount of waste generation from construction and packaging PS foam products in higher than 500000 tons per year, from which only 27% is recycled [1]. These very high numbers produce an important environmental issue, being necessary to find long-term solutions.

One of the most promising solutions is the substitution of non-biodegradable PS foams with biodegradable ones. Polylactide (PLA) is a biodegradable and biocompatible polymer produced from renewable sources such as cornstarch and sugarcane and it has been found to be the prefer substitute for non-biodegradable polymers [2,3]. PLA presents a great ability to degrade in the environment with a degradation half-time from six to two years in combination with its multifunction properties [4]. Thus, PLA is comparable to the commonly used polymers such as polypropylene (PP), polyethylene terephthalate (PET or PS, when talking about mechanical properties thermal or optical properties [5]. It has been proved to be insoluble in water, ethanol or methanol, and also presents aroma barrier and it is declared safe to be in contact with food [6]. Additionally, the high prize presenting since its discover has been reduced up to reasonable values to the polymer market. All these reasons make PLA the bioplastic with the widest window of applicability in comparison with other used bioplastics, such as cellulose based bioplastics, PHA or Starch-based bioplastics [7].

The wide range of applicability is due to the possibility of the fine control of its crystalline structure. PLA crystallizes in α, β *or* γ forms, being the α form the most stable and therefore the most common one. This phase has a 10_3 helical chain conformation and two chains in an orthorhombic unit cell. There exists an alteration of this α phase in which there exists some disorders in the chain named as α'. Depending of the crystalline phase, or the amount of each one, the properties suffers great changes, being therefore essential to understand and control the crystallinity behavior of PLA [8,9].

It applicability has been proved in several studies, it has been used in general packaging as well as in food and beverage packaging or biomedical applications such as scaffolds for tissue engineering [4,10,11]. In most of the applications the PLA is used as a cellular material. But these request a green foaming method, meaning that any organic solvent or residues coming from a chemical blowing agent can remain in the

* Corresponding author.
E-mail address: jmadeleon@fmc.uva.es (J. Martín-de León).

https://doi.org/10.1016/j.polymertesting.2021.107201
Received 13 January 2021; Received in revised form 27 March 2021; Accepted 11 April 2021
Available online 16 April 2021

foam after their production. For this reason, the use of carbon dioxide as a physical blowing agent has attracted significant attention for the production of PLA foams. Different technologies such as extrusion foaming [12–14], foam injection molding [15–17], and bead foaming [18–20] have been used to produce PLA foams using CO_2 as a physical blowing agent.

However, the production of foams using CO_2 is not a straightforward process. The physical reasons are connected with several effects taking place simultaneously, such as the plasticization of the polymer, the crystallization when the CO_2 is dissolved, the modifications of the crystallization and glass transition temperatures, and the effects of all these physical modifications of the polymer on the foaming mechanisms (nucleation, growth, and degeneration).

Some previous research works have been conducted on this topic. The presence of CO_2 has been proved to affect the crystallinity, the crystallization temperature, and the glass transition temperature (T_c and T_g) of PLA. Regarding crystallinity, it was proved that CO_2 affects PLA plasticity and the crystallization rate. Depending on the used pressure, a rise in solubility can lead to an increase in the final crystallinity or a decrease of it, affecting the final number of crystalline domains. Thus, Nofar et al. proved that when increasing the saturation pressure at which CO_2 is dissolved in PLA, from 0.1 MPa to 1.5 MPa, i.e., when increasing the solubility, in a range of saturation temperatures from 80 to 110 °C, crystallinity increases. However, when the pressure rises to 4.5 MPa, the final crystallinity decreases. The higher solubility enhanced by higher pressures leads to a higher nucleation rate of crystals; however, in the growing phase, this high amount of crystals leads to a less closed-packed structure and, as a consequence, to a smaller final crystallinity [21,22].

Crystallinity strongly determines the final cellular structure of PLA foams. A certain degree of crystallinity improves the polymer's visco-elasticity promoting cell nucleation and expansion [12,14,23]. However, if the crystallization degree is too high, the increase of the matrix's stiffness along with a smaller solubility will lead to a smaller expansion of the cellular material [24]. Additionally, crystallinity can promote heterogeneous nucleation, as far as spherulites can act as nucleation sites [25].

Crystallinity has been proved to be a critical factor in the final cellular structure of PLA foams for all the processing technologies previously mentioned. In extrusion foaming, in foam injection molding, and bead foaming, it has been proved that EPLA foam beads can be produced taking advantage of a double-crystal melting peak structure [19] with the same technology used for EPP [26].

Concerning the influence of CO_2 on T_c and T_g, both temperatures decrease in the gas's presence, affecting the previously described foaming methods [27,28].

Considering all previous results, it is evident that it is essential to measure and control the crystallization kinetics under CO_2 presence to handle the crystals' density and size and, consequently, to properly control the foam density, final number of cells, and its size. The crystallinity of PLA in the presence of pressurized CO_2 has been widely investigated through ex-situ techniques. Zhai et al. studied the crystallization and melting behaviors of linear PLA after being saturated with CO2 by using Differential Scanning Calorimetry (DSC) and Wide Angle X-Ray Diffraction (WAXD) [29]. Those ex-situ techniques give information about the final crystallinity of the material; however, it is difficult and time-consuming to extract information about what happens in the intermediate states, i.e., to measure the evolution of crystallinity with time. To solve this problem, it is necessary to employ in-situ techniques to monitor the crystallization kinetics. Related to this, Nofar et al. investigated the crystallization kinetics of three different PLAs employing a high-pressure DSC [30]. In this paper, the evolution of crystallinity with time was studied, extracting a high amount of information but only up to pressures of 6 MPa. In addition, in this research, it was not possible to analyze the spatial distribution of the CO2 dissolved in the samples as a function of time.

In the present study, a new technique for the in-situ characterization of the crystallization kinetics of PLA is proposed. An own-developed high-pressure vessel with windows has been used to measure the optical absorbance evolution of PLA under different CO_2 pressures. After calibration, this absorbance evolution allows quantifying the crystallinity during the whole process in a simple, quick, and non-destructive way. This new approach allows for the first time to follow the evolution of crystallinity not only with time but also allows obtaining results with spatial resolution (i.e., measuring the crystallinity evolution in different areas of the material). Moreover, using a pressure vessel enables widening the operating range up to saturation pressures and saturation temperatures, using samples of large dimensions compared to those used in high-pressure DSC, making the measurement approach more comparable to what happens when producing the foam. The paper aims to introduce this new approach and show several examples of its applicability for PLA.

2. Materials and methods

2.1. Materials

PLA Ingeo™ Biopolymer 2003D was kindly supplied in the form of pellets by Nature Works® LLC. The used material presents a density of 1.24 g/cm^3, with a molecular weight around 120.000 g/mol and a D-isomer of 3.5 wt %. The melt flow index (MFI) of this polymer has been measured to be 6 g/10 min (210 °C/2.16 Kg). The degree of crystallinity of this material is almost zero (Table 1) when it is processed by injection molding, extrusion, or compression molding.

Medical grade CO_2 (99.9% purity) was used for the gas dissolution experiments.

2.2. Methods

2.2.1. Precursors production

The as-received PLA was processed into sheets of 0.75 mm in thickness by following the next step. The pellets were first oven-dried at 50 °C for 12 h. Then, the material was processed into 0.13 mm thick sheets with a width of 100 mm through a single-screw extruder (Teach Line E 20 T) provided by Dr. Collin (Ebersberg, Alemania) (Fig. 1a). The pellets are put into in the hopper, introducing them into the extruder and make them advance at a rotation velocity of the screw of 60 rpm. The temperature profile in the barrel goes from 170 °C in the hopper to 190 °C in the die, increasing at intervals of 5 °C.

So as to perform the experiments, thicker precursor is required, so the obtained sheets are then laminated to obtain 0.75 mm sheets., by means of a cold/hot plate press (Talleres Remtex). The extruded sheets were cut so as to obtain 100 × 100 x 0.13 sheets. Six of those sheets were piled up and introduced inside a 0.75 mm in thick mould, between two aluminium foil and two steel plates (Fig. 1b). The whole system is later introduced in the hot plate of the press at 180 °C and under constant pressure of 2.2 MPa (Fig. 1d). Finally, the precursor was cooled down at 60 °C in the cold plates under the same pressure, and the 0.75 mm sheets was obtained.

These pieces were finally cut into 20 × 20 × 0.75 mm^3 samples in order to use them for the gas dissolution experiments.

2.2.2. Kinetics of crystallization

In order to follow the kinetics of crystallization of the PLA grade understudy and calibrate the optical measurements described in the next sections, an isothermal annealing was carried out. Nine different samples were annealed in a drying oven (Mod. E42, Heraeus) at 92 °C, and they were extracted at different times to measure its crystallinity and study the crystallinity evolution with time. Times from 0 to 70 min were used (see Table 1). It is essential to maintain the samples flat during the annealing because the optical properties of these materials need to be measured. To maintain the samples flat during annealing, they were located in between two flat steel sheets. The applied pressure was 66

Table 1
Characteristics of the samples for crystallinity-absorbance calibration.

Sample	Annealing Time (min)	Cold Crys. Temp. (°C)	Cold Crys. Enthalpy (J/g)	Melting Temp. (°C)	Melt. Enthalpy (J/g)	Crystallinity (%)	Abs. coeff (cm^{-1})
S1	0	122.0	23.4	153.9	−26.7	4.0	2.5
S2	10	110.3	20.2	153.3	−25.7	6.7	3.5
S3	15	107.4	16.9	153.2	−24.6	12.6	5.1
S4	20	106.3	14.2	154.3	−24.0	16.5	6.5
S5	25	106.2	11.6	153.3	−23.6	19.4	8.0
S6	30	104.1	9.2	153.6	−23.1	22.7	9.0
S7	40	104.6	5.8	152.9	−22.7	25.0	10.2
S8	50	–	–	153.6	−23.0	31.3	12.4
S9	70	–	–	153.3	−22.7	31.0	11.3

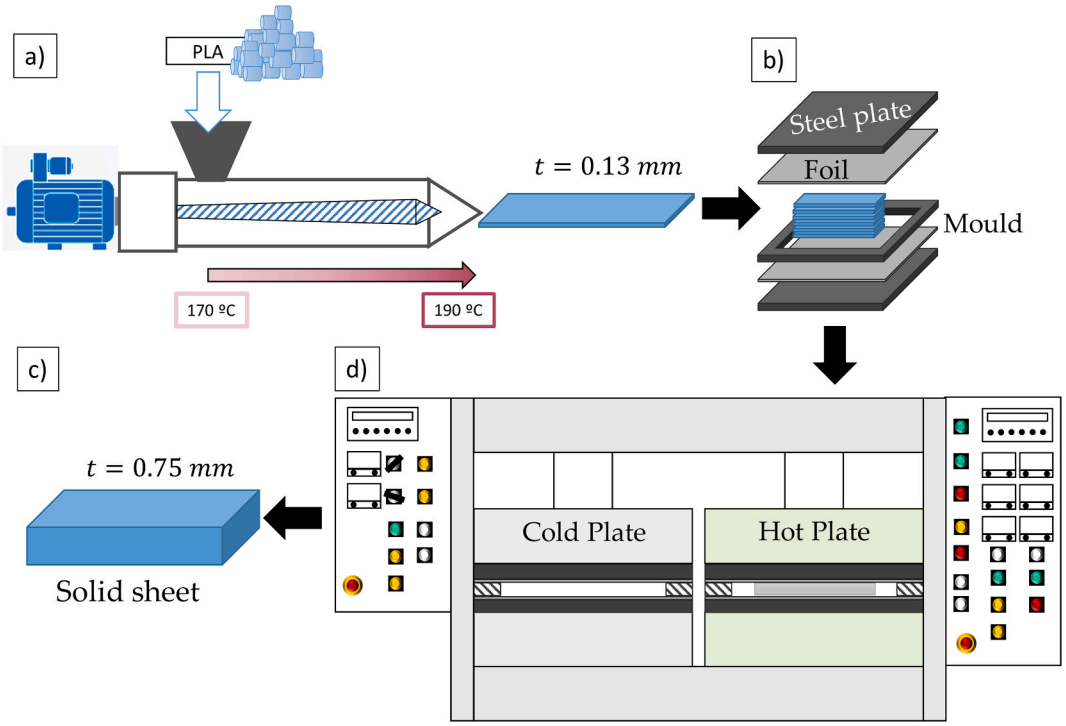

Fig. 1. Scheme of the precursor production process. a) Scheme of the extrusion process of the pellets into sheets 0.13 mm in thickness. b) Scheme of the system used to introduce the material in the press. c) Scheme of the plate press where the extruded sheets were laminated. d) Final solid sheet of 0.75 mm in thickness.

kPa.

2.2.3. Crystallinity

The crystallinity degree of the samples was measured by using a Mettler DSC30 differential-scanning calorimeter (Mettler-Toledo, Columbus, OH, USA) previously calibrated with indium. All measurements were performed from −20 °C to 220 °C at a heating rate of 10 °C/min. Some of the samples showed a cold crystallization peak [31], so the enthalpy of crystallization during heating ΔH_c and the melting enthalpy ΔH_m were measured, and the crystallinity (χ) was calculated as $[(\Delta H_m - \Delta H_c)/(\Delta H_f)]x100$ % where ΔH_f is the heat of fusion of a 100% crystalline material (93 J/g for 100% crystalline PLA [32]).

2.2.4. Set-up description

Gas dissolution experiments were performed in a set-up developed by our research team and schematize in Fig. 2.

The main part of this set-up is a high-pressure sight cell (**3**) schematized in more detail in Fig. 3. This pressure vessel is provided with eight locking screws (**4**) and can work up to 15 MPa of maximum pressure and 250 °C of temperature. Moreover, it is provided with a window of 60 mm (**5**), which allows observing inside the vessel.

The gas is provided to the system through an accurate pressure pump controller (model SFT-10) from Supercritical Fluid Technologies Inc. (Newark, DE, USA), which can work up to 68.9 MPa at a maximum flow rate of 24 ml/min. Temperature is controlled in the internal area of the pressure cell (Fig. 3). On the one hand, the heating is performed through a dual heating system of 400 W (**II**) connected to a temperature controller (CAL 3000). Additionally, the system comprises a cooling system (**V**) that can be connected to a chiller. Finally, the two heat interchangers (**IV**) allow better control of the working temperature.

The gas goes into the pressure vessel through the input valve (**1**) and goes out through a solenoid valve (**7**) that conducts the gas to a depressurization tank.

Additionally, the system is provided with several sensors allowing accurate data acquisition on a computer. The pressure sensor (Fig. 2 ((2)) measures the inner pressure, while the temperature acquisition is accomplished through three thermocouples inside the pressure vessel (Fig. 3 (I)). The first one controls the heating system, and two additional ones allow measuring the temperature at any point in the interior of the cell, the temperature of the gas and the temperature of the sample.

The sample holder (Fig. 3 (III)) is located between the two heating elements and allows introducing two samples simultaneously; the left one allows to visualize the thickness of the sample, while in the right one, the sample is situated facing the camera. In the experiments herein described, samples were situated in the right sample holder.

A collection of experiments has been carried out using this set up

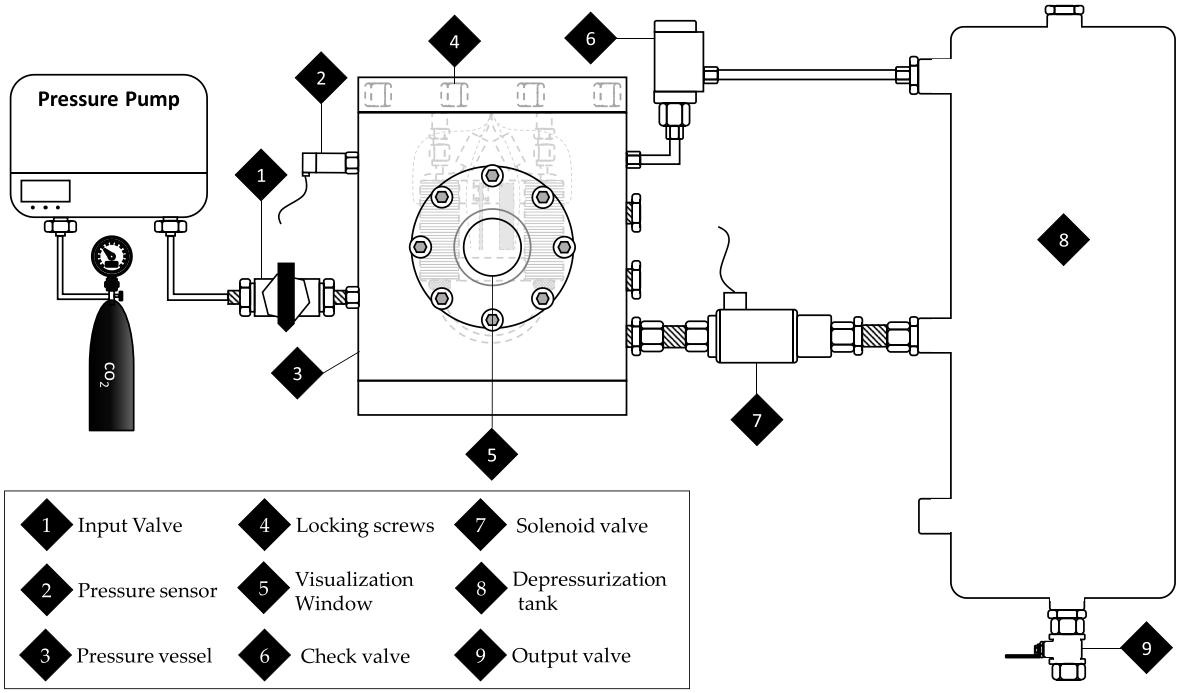

Fig. 2. Scheme of the used set-up for the gas dissolution experiments.

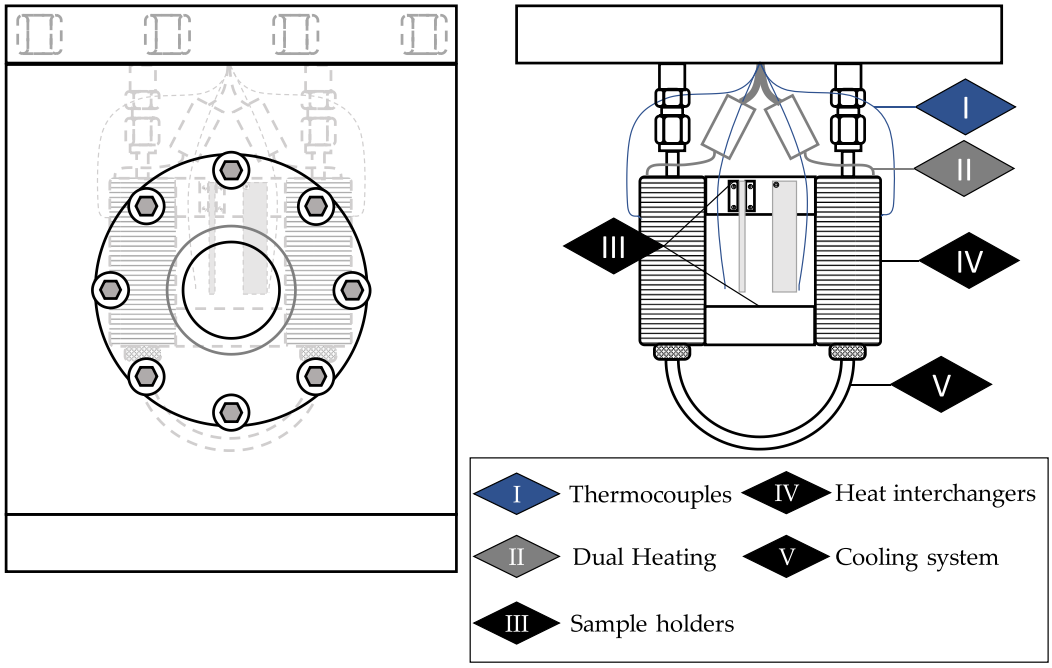

Fig. 3. Detail of the inside of the pressure vessel that allows controlling the temperature of the samples.

with a fixed temperature of 40 °C and pressures from 1.5 MPa to 4 MPa, as shown in Table 2. The conditions were selected with the idea of showing the potential of the technique presented in this paper. Samples were introduced in the pressure vessel under specific temperature and CO_2 pressure. At these conditions, gas diffuses inside the material, inducing some changes, such as crystallinity increase caused by the greater mobility of the polymeric chains [21]. These modifications can be visualized thanks to the pressure vessel window and analyzed as it is explained in the next section.

Table 2
Final characterization of the samples used for the dynamic crystallization tests.

Sample	Pressure vessel (MPa)	DSC Final Crystallinity (%)	Calibrated Final Crystallinity (%)	Relative error (%)
P1	1.5	5.9	5.7	3.4
P2	2.0	25.0	22.9	8.4
P3	2.5	23.7	23.7	0.0
P4	3.0	23.2	23.2	0.0
P5	3.5	24.2	24.6	1.6
P6	4.0	25.2	25.0	1.1

2.2.5. Transmittance measurements

Fig. 4a shows a scheme of another view of the set-up. A backlight led (**1**) homogeneously illuminated the sample. A high-resolution camera (16 bits; 1/60 fps UI-5480CP-M-GL model) (**3**), responsible for image acquisition, is situated in a holder able to move forward or backward so as to focus the image of the sample. Images were captured every 60 s during the whole experiments to study the samples' evolution with time.

Once the system is adjusted, optical images, as that shown in Fig. 4b showing a region of the sample (Fig. 5) can be obtained. Those images were processed using FIJI/ImageJ software. From those images, the grey level, proportional to light transmitted intensity, can be obtained and then related to optical magnitudes such as transmittance and absorbance. Transmittance is defined as the ratio between the transmitted (I) and the incident light (I_0), $T = (I/I_0)$. Thus, I_0 can be measured through the grey level of a region out of the sample (region 1 in Fig. 4), while I can be obtained through the grey level of a region inside the sample (region 2 in Fig. 2).

In order to being able to compare the measurements done at different conditions, background intensity was taken before each experiment with no samples inside the pressure vessel. This value was taken as the zero-grey level for each experiment and was later subtracted of each image.

This analysis allows obtaining both time and spatial resolution of the transmittance. The evolution of the material's overall transmittance can be obtained by selecting an area including almost the whole sample (Fig. 5a.) to measure I. Thus at a time t_1 the intensity of the whole selected *Region 2.1*$_1$ is considered as I_1 , while at a time t_2 this value has increased up to an overall intensity I_2 measured in *Region 2.1*$_2$ of the image. The analysis of this intensity through time leads to time resolution analysis. On the other hand, a grey level profile along the sample's width can be obtained considering regions such as region 2.2 in Fig. 4b and b. As it is schematized in Fig. 5b, the grey level changes through the width of the sample, creating an intensity profile. This profile evolves trough time as it can be seen for times t_1 and t_2 in Fig. 5b. The study of this evolution makes it possible to obtain the evolution of the transmittance with both time and spatial resolution.

Finally, the absorption coefficient of each sample can be calculated from the Beer-Lambert law as $\mu = -Ln(I/I_0)/t$, where t is the thickness of the sample (0.75 mm).

3. Results

3.1. Crystallinity-absorbance calibration

Light absorbance changes with crystallinity as it is shown in the following equation $A = \mu_c\chi + \mu_a(1-\chi)$, where (μ_a,μ_c)correspond to the optical absorption coefficients of the amorphous phase and the crystalline one, respectively. This means that polymers' transparency is reduced when crystallinity increases, i.e., the transmittance decreases, and absorbance increases.

So as to find the relationship between the optical properties and crystallinity, samples of PLA with a different final degree of crystallinity have been produced through annealing (see section 2.2.2). Afterward, their absorbance has been measured with the optical set-up described in section 2.2.5. Results are included in Table 1.

The different final degree of crystallinity was controlled through annealing under a constant temperature of 92 °C and a variable time from 10 to 70 min. Initially, precursors present a low crystallinity of 4.0% (measured by DSC). When the material is annealed under a specific temperature, the polymeric chains are able to reorganize, and therefore the crystallinity of the sample increases.

As Table 1 and Fig. 6 show, the crystallinity evolves from an initial value of 4% up to a maximum of 31% obtained when the annealing last more than 50 min. As shown in DSC curves, two peaks appear, one exothermic and another one endothermic, attributed to the cold-crystallization and crystal melting of PLA, respectively. At shorter annealing times, the cold crystallization peak presents significant importance, while, by increasing the annealing time, the area of this peak becomes smaller until it disappears at 50 min of annealing time. On the other hand, the area of the endothermic peak increases with annealing time. Both factors indicate the rise of the crystallinity as the annealing time increases.

The kinetics of crystallization can be studied by representing crystallinity evolution with time (Fig. 7a). It can be seen that crystallinity increases slowly at the beginning of the process; then, it rises to the maximum crystallinity that can be reached at those conditions for the PLA grade understudy.

After the annealing process, the absorption coefficient of the nine samples was measured. To do that, each sample was visualized with the U-eye camera inside the pressure vessel under atmospheric pressure and

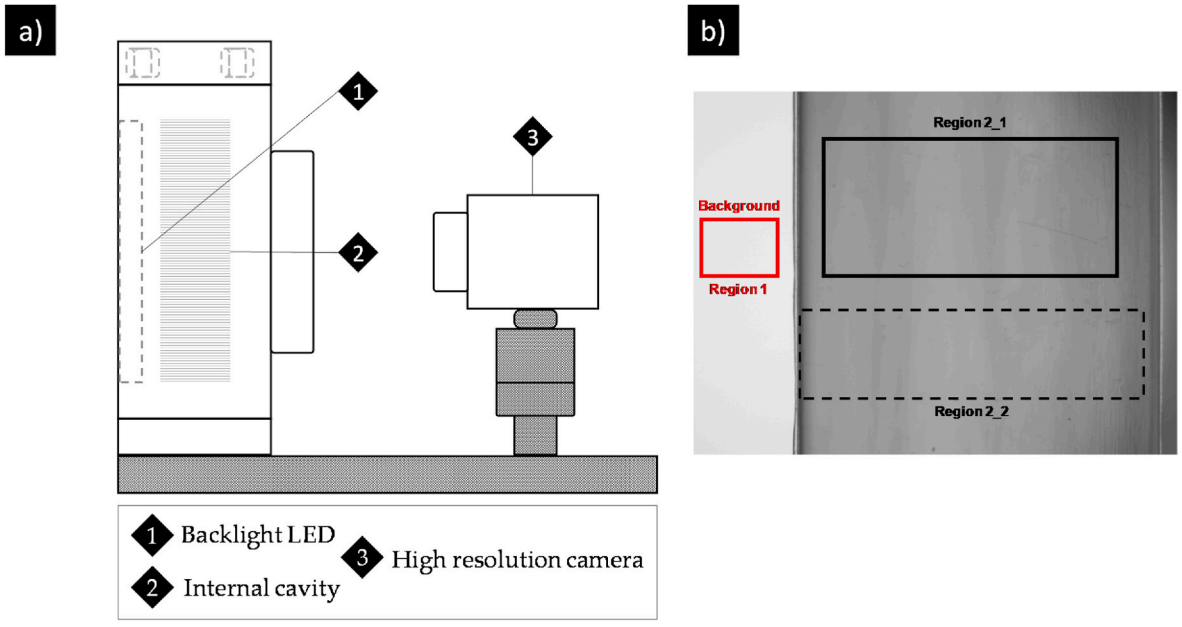

Fig. 4. a) Profile view of the pressure vessel along with the visualization camera. **b)** Example of an acquired image.

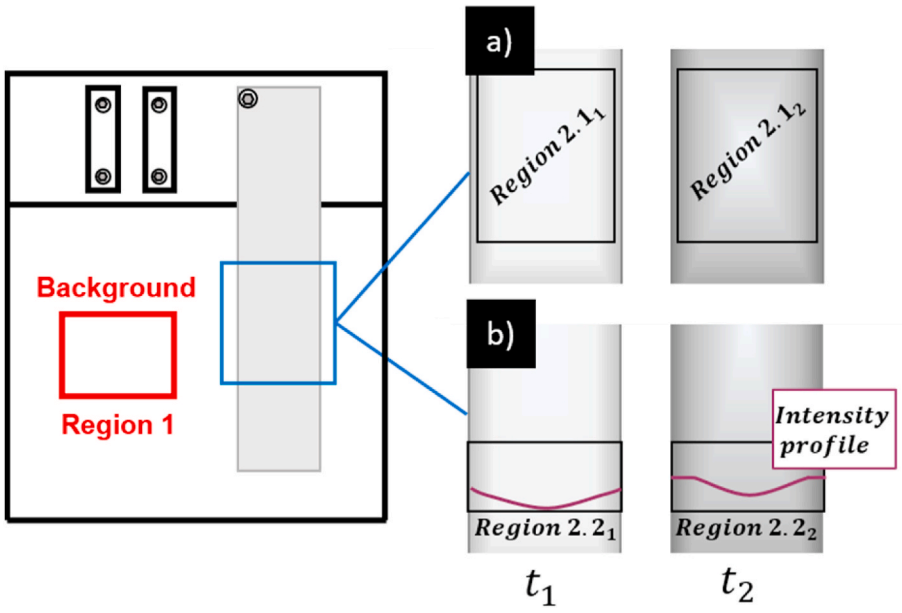

Fig. 5. Scheme of the different regions for transmittance analysis. a) with time resolution b) with time and spatial resolution.

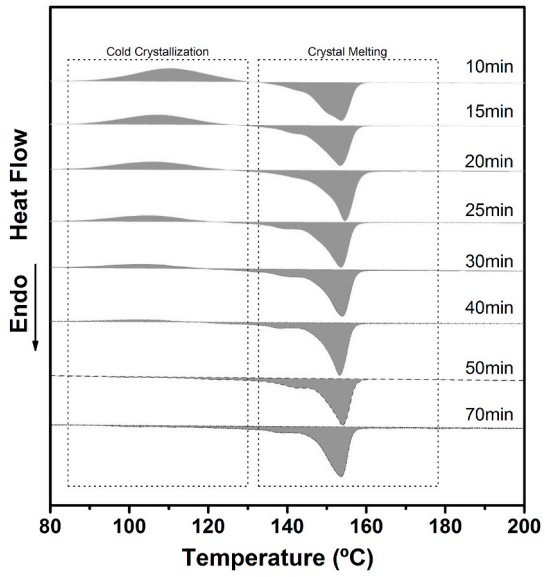

Fig. 6. Differential scanning calorimetry thermograms.

room temperature, measuring the absorbance of each one and calculating the absorption coefficient for each one.

It should be taken into account that the region of the sample used to measure the absorbance (region 2 in Fig. 4b) has been the same used for the DSC measurements.

As shown in Fig. 7a, the samples' absorption coefficient evolves with a similar trend to crystallinity. Samples with lower crystallinity degrees present an absorbance near zero, i.e., samples are mostly transparent. When crystallinity increases, samples become opaquer; that is, the absorbance and the absorption coefficient of the sample increases.

In conclusion, it has been proved that absorbance increases with crystallinity, so these two magnitudes can be correlated. When the absorption coefficient is represented as a function of crystallinity, linear regression with a high correlation coefficient ($R^2 = 0.99$) is obtained, as shown in Fig. 7b. This correlation has been used as a calibration curve that allows determining the crystallinity of the sample by measuring the absorbance.

It is also possible to obtain the optical absorption coefficients (μ_a, μ_c)associated with the amorphous and crystalline parts using the obtained calibration. Since $A = \mu_c\chi + \mu_a(1-\chi)$ it is obtained that $\mu_a = 1.00cm^{-1}$ and $\mu_c = 36.15cm^{-1}$. This shows that the crystalline part of PLA scatters much more light than the amorphous part, as expected.

3.2. *In-situ evolution of absorbance/crystallinity*

The described set up for gas dissolution foaming, along with the previously described calibration, allows to in-situ obtain the crystallinity's evolution with both time and spatial resolution when PLA is exposed to pressurized CO_2.

Samples crystallized under six different conditions were studied (Table 2). Diffusion of gas inside the polymer is a slow process, so it is crystallization kinetics.

As it is shown in Fig. 8a, by analyzing the mean absorption coefficient of the whole sample through time, it was possible to obtain the time evolution of the total crystallinity of PLA under different CO_2 pressures. On the other hand, the study of the absorption coefficient profile along the sample's width leads to obtain the crystallinity profile in the sample and its time evolution (Fig. 8b).

Regarding the evolution of the total crystallinity, it can be seen that the used CO_2 pressure strongly influences the crystallization kinetics. On the one hand, a small pressure of 1.5 MPa does not trigger crystallization even for long times. On the other hand, it can be seen how an increase of the pressure from 2 to 4 MPa leads to faster kinetics of crystallization. PLA crystallizes under CO_2 pressure due to the plasticization effect. That means that the presence of gas decreases the glass transition temperature of the polymer, and therefore molecular mobility increases. Thus, when using 1.5 MPa, the solubility of the gas inside PLA is so small that this plasticization effect is almost negligible. Simultaneously, increasing pressure leads to a higher solubility, a higher plasticization effect, and, therefore, higher molecular mobility that allows a faster reorganization.

However, the final crystallinity of the samples is almost constant (Table 2). This was previously observed for PLA under a CO_2 atmosphere. The final crystallinity would be influence by both crystal nucleation and growth kinetics. A higher pressure promotes more significant nucleation but also faster growth of crystals, meaning that the formed crystals are less perfect and less packed, influencing negatively the final crystallinity. For smaller pressures besides smaller nucleation, a slower-growing allows the formation of more perfect and packed

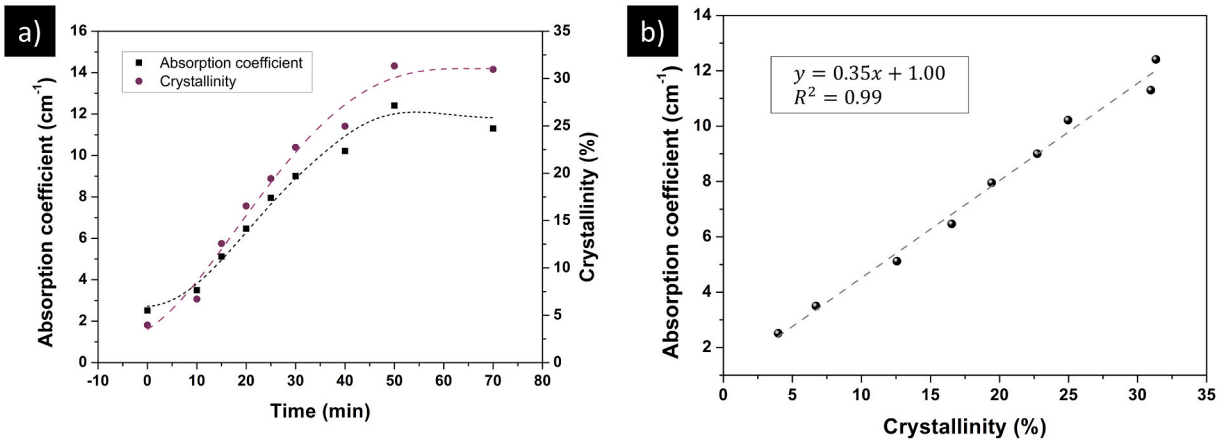

Fig. 7. a) Absorbance and crystallinity curves as a function of time. b) Correlation between absorbance and crystallinity.

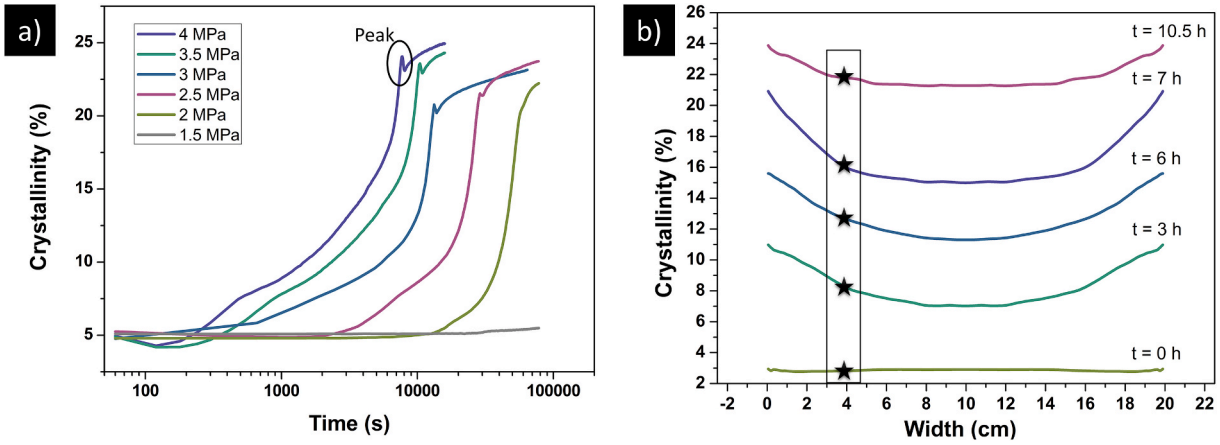

Fig. 8. a) Evolution of crystallinity with time for the whole sample. A crystallinity peak is marked in the 4 MPa curve. b) Time evolution of crystallinity along the width of a PLA sample under 2.5 MPa of CO_2 pressure and 40 °C of temperature. Stars mark the selected points to follow the crystallinity evolution with time in a selected point of the sample.

crystals [33].

This final value of crystallinity calculated through the proposed method, "calibrated final crystallinity," was compared with the one obtained through DSC of the samples after the dissolution experiments. As it is shown in Table 2, the relative error between the measurements is remarkably low, especially at pressures larger than 2 MPa (less than 1%), highlighting the reliability of the proposed method.

Regarding the evolution of the crystallinity profile in the samples, it can be explained through the diffusion mechanism of CO_2. Diffusivity of CO_2 inside PLA follows the second Fick equation [34]. When considering a plane sheet, the solution of this equation leads to diffusion profiles similar to the crystallization profiles observed in Fig. 8b. Crystallinity evolution depends on CO_2 concentration; this is always higher in the edges of the sample, so it is crystallinity evolution. As gas diffuses into the sample, crystallinity grows and homogenizes up to CO_2 saturation. Thus when the diffusion experiment starts ($t = 0$), the sample presents a constant crystallinity in all the thickness around 3%. As CO_2 diffuses inside the sample, solubility increases showing a strong profile, with a higher amount of gas in the edges that gradually reduces up to the center of the sample (10 mm in Fig. 8b). As explained, crystallinity evolves simultaneously with solubility, so after 3 h of gas diffusion, crystallinity in the sample's edges is around 11%, a value that gradually decreases up to 7% in the center of the sample. This difference is even significant after a larger diffusion time. After $t = 7\ h$ crystallinity in the edges approaches to the maximum reached crystallinity showing a value of 21%, while in the center the value is around 15%. Crystallinity profile becomes smother up to solubility is the maximum along the thickness leading to a maximum crystallinity of 24% in the whole sample.

Crystallization kinetics can also be in-depth analyzed through the Avrami equation (1) with the presented technique. Considering the obtained time evolution crystallinity curves obtained (Fig. 8b), it is possible to follow the crystallinity evolution at any point of the sample thickness as shown in Fig. 8b, only by selecting the same thickness point for the different crystallinity curves. From those crystallinity values, the kinetics of crystallization can be described through Equation (1):

$$\ln(-\ln(1-\chi(t)) = nlnt + lnk \tag{1}$$

Where $\chi(t)$ is the crystallinity, t is the time, n is the Avrami exponent, and k is the crystallization kinetic constant.

As it can be seen in Fig. 9, two different crystallization regimes can be defined for this experiment, where the Avrami exponent evolves from 1.17 to 3.15. The Avrami exponent can be split into two terms:

$$n = n_d + n_n \tag{2}$$

Where n_d takes into account the dimensionality of the growing crystals, being 1, 2, or 3, the possible values corresponding to the dimensions of the formed crystals. And n_n represents the time dependence of the nucleation, where 0 indicates that the nucleation is instantaneous or heterogeneous and one corresponds to sporadic or homogeneous nucleation. However, the nucleation can be between completely instantaneous or completely sporadic, finding a non-integer Avrami

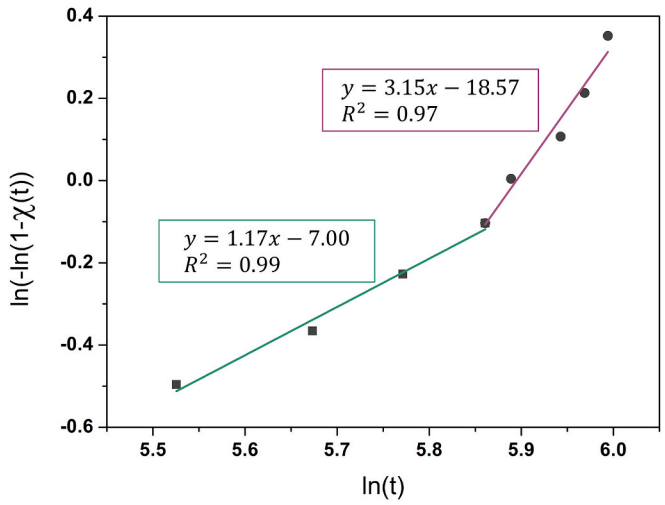

Fig. 9. Avrami double-log plots of PLA crystallization at 2.5 MPa of CO_2 pressure and 40 °C of temperature.

exponent.

Taking this into consideration, the Avrami analysis in Fig. 9 seems to indicate during the first part of the diffusion experiment, crystals grow unidimensionally from instantaneous nucleation. This situation evolves when solubility increases, leading to a three-dimensional growth of the crystal that means a spherulitic growth.

At last, an important aspect must be mentioned. The absorbance curves show an unexpected peak before the maximum reached value (Fig. 8a), and therefore after calibration, this peak is observed in crystallinity graphs.

This peak seems to be associated with the diffusion mechanisms of CO_2 and not with an instantaneous growth in crystallinity. When talking about gas diffusion in a semi-crystalline polymer, gas-philicity in crystalline domains is very low. It can be then considered that sorption is only taking place in the amorphous part. In this amorphous part, gas diffuses both through the polymeric matrix (absorption) and through the free volume of the polymer (adsorption).

As it was previously commented, only the amorphous part is capable of absorbing gas. When the gas reaches the center of the sample (Fig. 10), crystallization is promoted in the material's whole thickness. So, the gas located in the amorphous part that is crystallizing precipitates suddenly, leading to an increase in the sample's grey level. After this rapid increase, the gas distributes again through the matrix and the free volume.

4. Conclusions

It has been proved that it is possible to measure the crystallization kinetics of Polylactic Acid in the presence of CO_2 using a non-destructive optical approach consisting of measuring the optical absorbance of the polymer when it is located in a pressure vessel under specific pressure of this gas. This approach allows determining the kinetics of crystallization in a non-destructive way with both time and spatial resolution and large samples compared to those used for high-pressure DSC techniques.

Studying absorbance's evolution, it has been found that the presence of CO_2 inside the polymer matrix triggers the crystallization in PLA due to the plasticization effect of this gas that allows the reorganization of the polymer chains into a more stable state.

To show the potential of this approach, the kinetics of crystallization at 40 °C and different pressures have been studied, finding that there is a minimum pressure of 1.5 MPa, below which the crystallization does not start. When this pressure is reached, crystallinity increases with saturation pressure, and so does the rate of the process.

Finally, the experimental data crystallinity vs. time presents a non-expected peak that has been associated with the diffusion mechanisms of CO_2 inside the polymer. When the gas reaches the center of the sample, it is postulated that it promptly precipitates. This precipitation can be attributed to a reduction in both the absorption or the adsorption mechanisms. After the first instants, gas can diffuse into the polymer again, recovering the absorption curve its expected shape.

The methodology presented in this paper can be extended to the detailed analysis of other polymers in which similar phenomena take place.

Financial support

Financial assistance from the Junta of Castile and Leon (VA202P20) and Spanish Ministry of Science, Innovation, and Universities (RTI2018-098749-B-I00 and RTI2018-097367-A-I00) and the "Ente Público Regional de la Energía de Castilla y León" (EREN) are gratefully acknowledged. Financial support from the Junta of Castile and Leon grant (J. Martín-de León) is gratefully acknowledged.

The raw/processed data required to reproduce these findings cannot be shared at this time due to technical or time limitations.

Author statement

Judith Martín-de León: Methodology, Validation, Formal analysis,

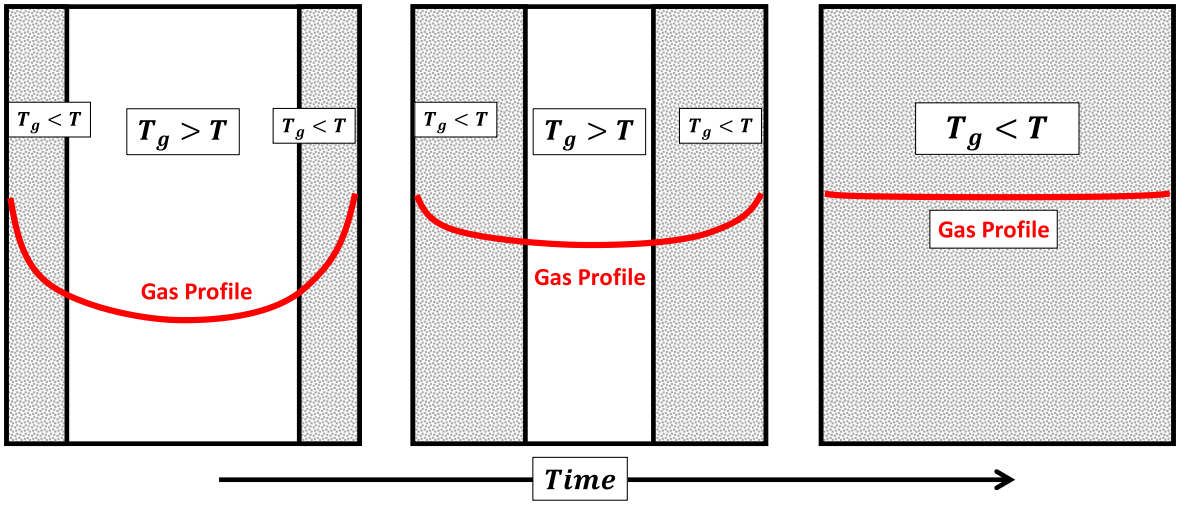

Fig. 10. Scheme of the evolution of Tg during diffusion experiment.

Investigation, Data curation, Writing – original draft, writing-review ¬editing. Victoria Bernardo: Investigation, Data curation, writing-review ¬editing. Eusebio Solórzano: Conceptualization, Methodology, Software, Investigation, Supervision. Miguel Ángel Rodriguez-Pérez: Conceptualization, Methodology, Supervision, writing-review ¬editing, Project administration, Funding acquisition.

Declaration of competing interest

The authors declare that they have no known competing financial interests or personal relationships that could have appeared to influence the work reported in this paper.

References

[1] C. Lassen, M. Warming, L.G. Jakobsen, B. Novichkov, J. Strand, L. Feld, L. Bach, Survey of polystyrene foam (Eps and Xps) in the Baltic Sea, Danish fish. Agency/minist, Environ. Food Denmark (2019).

[2] L.T. Lim, R. Auras, M. Rubino, Processing technologies for poly(lactic acid), Prog. Polym. Sci. 33 (2008) 820–852, https://doi.org/10.1016/j.progpolymsci.2008.05.004.

[3] M. Nofar, A. Ameli, C.B. Park, Development of polylactide bead foams with double crystal melting peaks, Polymer 69 (2015) 83–94, https://doi.org/10.1016/j.polymer.2015.05.048.

[4] G.E. Luckachan, C.K.S. Pillai, Biodegradable polymers- A review on recent trends and Emerging perspectives, J. Polym. Environ. 19 (2011) 637–676, https://doi.org/10.1007/s10924-011-0317-1.

[5] N.H. Yusoff, K. Pal, T. Narayanan, F.G. de Souza, Recent trends on bioplastics synthesis and characterizations: polylactic acid (PLA) incorporated with tapioca starch for packaging applications, J. Mol. Struct. 1232 (2021) 129954, https://doi.org/10.1016/j.molstruc.2021.129954.

[6] DuPont, Food and Beverage Packaging Materials, 2016, p. 2016.

[7] A. Folino, A. Karageorgiou, P.S. Calabrò, D. Komilis, Biodegradation of wasted bioplastics in natural and industrial environments: a review, Sustain. Times 12 (2020) 1–37, https://doi.org/10.3390/su12156030.

[8] M. Puchalski, S. Kwolek, G. Szparaga, M. Chrzanowski, I. Krucinska, Investigation of the influence of PLA molecular structure on the crystalline forms (α" and α) and Mechanical Properties ofWet Spinning Fibres, Polymers 9 (2017), https://doi.org/10.3390/polym9010018.

[9] F. Foglia, A. De Meo, V. Iozzino, V. Volpe, R. Pantani, Isothermal crystallization of PLA: nucleation density and growth rates of α and α' phases, Can. J. Chem. Eng. (2020) 1998–2007, https://doi.org/10.1002/cjce.23818.

[10] R.K. Meszlenyi, A.G. Mikos, P. D, of poly (DL-lactic-co-glycolic acid) foam scaffolds, Tissue Eng. 5 (1999) 421–433.

[11] A.G. Mikos, M.D. Lyman, L.E. Freed, R. Langer, Wetting of poly(l-lactic acid) and poly(dl-lactic-co-glycolic acid) foams for tissue culture, Biomaterials 15 (1994) 55–58, https://doi.org/10.1016/0142-9612(94)90197-X.

[12] M. MIhai, M.a. Huneault, B.D. Favis, Rheology and extrusion foaming of chain-branched poly(lactic acid), Polym. Eng. Sci. 50 (2009), https://doi.org/10.1002/pen.

[13] S. Pilla, S.G. Kim, G.K. Auer, S. Gong, C.B. Park, Microcellular extrusion-foaming of polylactide with chain extender, Polym. Eng. Sci. 49 (2009), https://doi.org/10.1002/pen.

[14] J. Wang, W. Zhu, H. Zhang, C.B. Park, Continuous processing of low-density, microcellular poly(lactic acid) foams with controlled cell morphology and crystallinity, Chem. Eng. Sci. 75 (2012) 390–399, https://doi.org/10.1016/J.CES.2012.02.051.

[15] T. Ishikawa, T. Kentaro, M. Ohshima, Visual observation and numerical studies of N2 vs. CO2 foaming behavior in core-Back foam injection molding, Polym. Eng. Sci. 52 (2006), https://doi.org/10.1002/pen.

[16] A. Kramschuster, S. Gong, L.-S. Turng, T. Li, T. Li, Injection-molded solid and microcellular polylactide and polylactide nanocomposites, J. Biobased Mater. Bioenergy 1 (2008) 37–45, https://doi.org/10.1166/jbmb.2007.004.

[17] A. Kramschuster, L.S. Turng, An injection molding process for manufacturing highly porous and interconnected biodegradable polymer matrices for use as tissue engineering scaffolds, J. Biomed. Mater. Res. B Appl. Biomater. 92 (2010) 366–376, https://doi.org/10.1002/jbm.b.31523.

[18] C.B. Park, M. Nofar, METHOD FOR THE PREPARATION OF PLA BEAD FOAMS, 2018.

[19] M. Nofar, Expanded PLA Bead Foaming: Analysis of Crystallization Kinetics and Development of a Novel Technology, 2013.

[20] M. Nofar, Y. Guo, C.B. Park, Double crystal melting peak generation for expanded polypropylene bead foam manufacturing, Ind. Eng. Chem. Res. 52 (2013) 2297–2303, https://doi.org/10.1021/ie302625e.

[21] M. Nofar, W. Zhu, C.B. Park, Effect of dissolved CO2 on the crystallization behavior of linear and branched PLA, Polymer 53 (2012) 3341–3353, https://doi.org/10.1016/j.polymer.2012.04.054.

[22] M. Nofar, C.B. Park, Poly (lactic acid) foaming, Prog. Polym. Sci. (2014), https://doi.org/10.1016/j.progpolymsci.2014.04.001.

[23] M. MIhai, M.a. Huneault, B.D. Favis, Crystallinity development in cellular poly (lactic acid) in the presence of Supercritical carbon dioxide, J. Appl. Polym. Sci. 113 (2009) 2920–2932, https://doi.org/10.1002/app.

[24] C. Marrazzo, E. Di Maio, S. Iannace, Conventional and nanometric nucleating agents in poly(e-caprolactone) foaming: crystals vs. Bubbles nucleation, Polym. Eng. Sci. 48 (2007), https://doi.org/10.1002/pen.

[25] K. Taki, D. Kitano, M. Ohshima, Effect of growing crystalline phase on bubble nucleation in poly(L -lactide)/CO2 batch foaming, Ind. Eng. Chem. Res. 50 (2011) 3247–3252, https://doi.org/10.1021/ie101637f.

[26] J.B. Choi, M.J. Chung, J.S. Yoon, Formation of double melting peak of poly (propylene-co-ethylene-co-1-butene) during the preexpansion process for production of expanded polypropylene, Ind. Eng. Chem. Res. 44 (2005) 2776–2780, https://doi.org/10.1021/ie0401399.

[27] M. Takada, S. Hasegawa, M. Ohshima, Crystallization kinetics of poly(L-lactide) in contact with pressurized CO2, Polym. Eng. Sci. 44 (2004) 186–196, https://doi.org/10.1002/pen.20017.

[28] L. Yu, H. Liu, K. Dean, Thermal behaviour of poly(lactic acid) in contact with compressed carbon dioxide, Polym. Int. 58 (2009) 368–372, https://doi.org/10.1002/pi.2540.

[29] W. Zhai, Y. Ko, W. Zhu, A. Wong, C.B. Park, A study of the crystallization, melting, and foaming behaviors of polylactic acid in compressed CO2, Int. J. Mol. Sci. 10 (2009) 5381–5397, https://doi.org/10.3390/ijms10125381.

[30] M. Nofar, W. Zhu, C.B. Park, Effect of dissolved CO2 on the crystallization behavior of linear and branched PLA, Polymer 53 (2012) 3341–3353, https://doi.org/10.1016/j.polymer.2012.04.054.

[31] D. Wu, L. Wu, L. Wu, B. Xu, Y. Zhang, M. Zhang, Nonisothermal cold crystallization behavior and kinetics of polylactide/clay nanocomposites, Appl. Polym. Sci. 45 (2007) 1100–1113, https://doi.org/10.1002/polb.

[32] E.W. Fischer, H.J. Sterzel, G. Wegner, Investigation of the structure of solution grown crystals of lactide copolymers by means of chemical reactions, Kolloid-Z. Z. Polym. 251 (1973) 980–990, https://doi.org/10.1007/BF01498927.

[33] M. Nofar, A. Tabatabaei, C.B. Park, Effects of nano-/micro-sized additives on the crystallization behaviors of PLA and PLA/CO 2 mixtures, Polymer 54 (2013) 2382–2391, https://doi.org/10.1016/j.polymer.2013.02.049.

[34] S. Siripurapu, J.a. Coughlan, R.J. Spontak, S.a. Khan, Surface-constrained foaming of polymer thin films with Supercritical carbon dioxide, Macromolecules 37 (2004) 9872–9879, https://doi.org/10.1021/ma0484983.